J Clust Sci (2013) 24:945–958
DOI 10.1007/s10876-013-0580-5

ORIGINAL PAPER

Theoretical Studies of the Electronic Structures and Spectrum Properties of Pt_nNi_m ($n + m = 7$, n, $m \neq 0$) Clusters

Xiu-Rong Zhang · Fu-Xing Zhang · Xing Yang · Ai-Hua Yuan

Received: 30 November 2012 / Published online: 4 June 2013

Abstract We studied Pt_nNi_m ($n + m = 7$, n, $m \neq 0$) clusters within the framework of the density functional theory (B3LYP) at the LANL2DZ level. The calculated results show that the Fermi levels are determined by the number of Pt atoms, which gain electrons from Ni atoms. Meanwhile, multifarious orbital hybridization is found in the frontier molecular orbital, and the more platinum or nickel atoms, the smaller energy gap it has. Moreover, the calculated IR and Raman spectrum indicates the aromatic character, which is vital for transitional metal clusters.

Keywords Pt_nNi_m ($n + m = 7$, n, $m \neq 0$) clusters · Electronic structure · Spectrum and aromatic properties · Density functional theory

PACS Nos. 36.40.Cg · 36.40.Vz · 71.15.Mb

Introduction

Bimetallic clusters, composed of two different metal elements, are of greater interest than monometallic ones for the improvement of catalytic properties of metal

X.-R. Zhang (✉)
School of Mathematics and Physics, Jiangsu University of Science and Technology, Zhenjiang 212003, Jiangsu, People's Republic of China
e-mail: zh4403701@126.com

F.-X. Zhang · X. Yang
School of Materials Science and Engineering, Jiangsu University of Science and Technology, Zhenjiang 212003, Jiangsu, People's Republic of China
e-mail: zfx611319@hostmail.com

A.-H. Yuan
School of Biology and Chemical Engineering, Jiangsu University of Science and Technology, Zhenjiang 212003, Jiangsu, People's Republic of China

particles. The huge advantage of bimetallic clusters is that their properties may be tuned by varying not only their size and geometries, but also their composition [1]. Recently, platinum alloyed with some 3*d* transition metal clusters have been aroused considerable interests by chemists and physicists due to their unique physical and chemical properties, particularly, their superior catalytic activities for a number of reactions. It has been demonstrated that when Pt is alloyed with transition metals such as Cr, Mn, Fe, Co and Ni, a two- to fourfold improvement in oxygen reduction reaction (ORR) activity, compared with a Pt catalyst, could be achieved [2–8]. Recently, more and more research interests have been devoted to study the intrinsic mechanics of high catalytic activity by Pt alloy. For example, Stamenkovic et al. [9] studied polycrystalline alloy films of Pt_3M catalysts (M = Ni, Co, Fe and Ti) to understand the role of 3*d* metals in the electro-catalytic ORR activity of Pt-alloys. They found that in these Pt_3M alloys, the catalytic activity for the ORR was dependent on the nature of the 3*d* metal, where the Ni, Co and Fe alloys were much more active than pure Pt, while others exhibited less enhancement. Antolini et al. [10] investigated the relationship between the stability of alloyed clusters, using $Pt_{1-x}M_x$ (M = Fe, Ni and Co). They found that when x was small, only the unalloyed base metal could be dissolved. However, if x was increased to 0.6, even an alloyed metal could be dissolved from the bulk alloy.

Additionally, there are several first-principles calculations of the electronic structures of Pt alloyed with 3*d* transition metal systems. Nørskov et al. [11] studied nanoscale effects on electro-catalytic activity using density functional theory (DFT) calculations and showed that alloys of Pt and, for example, Ni, Co, Fe and Cr (where Pt is segregated on the surface) have smaller oxygen binding energies than pure Pt. These results provided good explanations for experimental observations that the Pt skins on these alloys have higher catalytic activity than pure Pt. Kootte et al. [12] performed spin-polarized band structure calculations of Co_xPt_{1-x} alloys with $x = 0$, 0.25, 0.5, 0.75, and 1, and reported density of states and magnetic moments of the clusters. Xiong and Manthiram [13, 14] claimed that alloys with ordered structures might further enhance catalytic activity by optimizing several factors, such as (i) the geometric and electronic structure of Pt, for the optimum number of base metal atoms as nearest neighbours, (ii) *d*-electron density in Pt atomic surface configuration, and (iii) Pt–Pt distance.

Our group have already successfully completed the investigation on the geometric structure, spectrum, electronic and magnetic properties of Pt_nNi_m ($n + m \leq 5$, $n, m \neq 0$) [15] and Pt_nNi_m ($n + m = 6$, $n, m \neq 0$) cluster [16]. In order to make a thorough inquiry into the regularity for change of structure and properties of Pt–Ni bimetallic cluster as enhancing its size scale, the geometric structure, stability and magnetic moments of Pt_nNi_m ($n + m = 7$, $n, m \neq 0$) cluster [17] were investigated lately, and in this paper we will perform systematic calculations on these cluster sequentially, the ground state structure, orbital energy level, natural bond orbital (NBO) charge populations, infrared (IR) and Raman spectrum, and aromatic properties of the Pt_nNi_m ($n + m = 7$) cluster, which provides a good way to understand the Pt–Ni bimetallic cluster.

Computational Details

The geometric structures, electronic and spectroscopy properties of Pt_nNi_m ($n + m = 7$, n, $m \neq 0$) cluster were calculated by using all-electron DFT implemented in the Gaussian 03 package [18]. We used the unrestricted B3LYP exchange–correlation potential and employed the relativistic 19-electron Los Alamos National Laboratory (LANL2DZ) effective core pseudopotentials [19] with the basis sets (3*s*3*p*2*d*), which provide an effective way to reduce difficulties in calculations of two-electron integrals caused by heavy transition metal atoms. We confirm the stability of the lowest-energy structures as minima of the potential energy surface by considering vibrational frequency. Our previous computations [20–22] on the W_n clusters have shown that the B3LYP and B3PW91 functions can provide reliable qualitative results. For the Pt_nNi_m ($n + m = 7$) clusters system, In order to compare with the available experimental values and previous theoretical works, we calculate the bond lengths, vibrational frequencies, and binding energy of Pt_2 clusters in our methods and the results show that the bond lengths is 2.376 Å, vibrational frequencies is 234.5 cm^{-1} and binding energy is 3.24 eV, which are in excellent agreement with available experiment data [23–25], 2.333 Å, 222.5 cm^{-1} and 3.14 eV, respectively. These indicate that our methods are reliable and accurate enough to describe the structures and properties of Pt_nNi_m ($n + m = 7$) clusters.

Results and Discussion

Geometrical Structure

In order to find out the lowest-energy structures of Pt_nNi_m ($n + m = 7$, n, $m \neq 0$) clusters, we consider a great quantity of initial configurations, which are likely to be stable. In the calculated results, the structures with no virtual frequency are regarded as stable structures. The structure with the lowest-energy and no virtual frequency is appointed as the ground state structure. Figure 1 depicts the ground state structures of Pt_nNi_m ($n + m = 7$) clusters, where a deep color sphere refers to Pt atom and light color sphere is Ni atom. As can be seen from the Fig. 1 and Table 1, all the structures of Pt_nNi_m ($n + m = 7$) clusters are three-dimensional structure, with low symmetry and high spin-multiplicity (SM). Because the impurity atom is imported, the ground structures of Pt_nNi_m ($n + m = 7$, n, $m \neq 0$) clusters are greatly changed, compared with pure metal clusters [26, 27]. The ground state structure of Pt_1Ni_6 cluster is an irregular pentagonal bipyramid structure, whose electronic state is $7A'$, while the Pt_6Ni_1 cluster is a little distorted coupled tetragonal pyramid structure, whose electronic state is $7A''$; The ground state structure of Pt_2Ni_5 cluster is a quadrangle-capped prism structure, whose electronic state is $9A'$, while the Pt_5Ni_2 cluster is a malposed coupled tetragonal pyramid structure, whose electronic state is 5A. The ground state structure of Pt_3Ni_4 cluster is a distorted coupled tetragonal pyramid structure, whose electronic state is $7A''$, while the Pt_5Ni_2 cluster is a three triangle-capped triangle pyramid structure, whose electronic state is $7A'$.

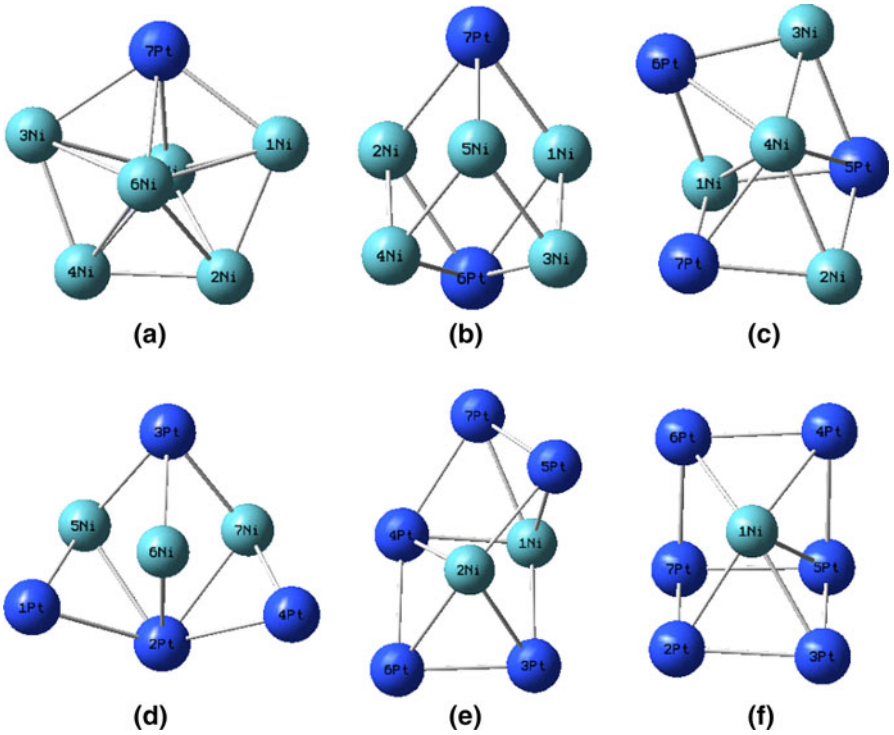

Fig. 1 The ground state of Pt_nNi_m ($n + m = 7$, n, $m \neq 0$) clusters

The symmetry of all the Pt_nNi_m ($n + m = 7$) clusters is C_s, excluding the Pt_5Ni_2 cluster is C_2 symmetry.

Energy Level Analysis

The electrons of the metal atom could be seen as free electrons in piece of metal solid, the energy spectrum of which are continuous spectral band. However, as to the small metal cluster, the energy spectra are noncontinuous spectral band, the character of which is separated energy level. When an electron absorbs a photon, the electron transition from low to high energy level in cluster can occur. Moreover the intervals of energy level respond to changes in the size of cluster. Figure 2 shows the molecular orbital energy levels of Pt_nNi_m ($n + m = 7$, n, $m \neq 0$) clusters around the fermi level. We can not ignore the effect of spin-polarized state on the ground state structure, so the energy level contains two sets of level (α- and β-states). In Fig. 2, the 'up' and 'down' represent the α-states and β-states, respectively. Normally, HOMO level is the larger one between the up state and down state, LUMO level is the lower one between the up state and down state. Fermi level is the median between the HOMO and LUMO level. Energy gap is the differential between LUMO and HOMO. If the HOMO and LUMO belong to the same up or down state, the energy gap is direct energy gap, or else, the energy gap is

Table 1 The structure (STR), symmetry (SYM), spin multiplicity (SM), electronic state (ES), HOMO, LUMO, fermi level (FL), energy gap (EG) and total magnetic moments (MM) of the ground state structures of Pt_nNi_m ($n + m = 7$, $n, m \neq 0$) clusters

Cluster	STR	SYM	SM	ES	HOMO (eV)	LUMO (eV)	FL (eV)	EG (eV)	MM (μ_B)
Pt_1Ni_6	a	C_s	7	$^7A'$	−4.653	−3.456	−4.054	1.197	6
Pt_2Ni_5	b	C_s	9	$^9A'$	−4.952	−3.374	−4.163	1.578	8
Pt_3Ni_4	c	C_s	7	$^7A''$	−5.306	−3.265	−4.286	2.041	6
Pt_4Ni_3	d	C_s	7	$^7A'$	−5.279	−3.565	−4.422	1.714	6
Pt_5Ni_2	e	C_2	5	^5A	−5.633	−3.973	−4.803	1.660	4
Pt_6Ni_1	f	C_s	7	$^7A''$	−5.606	−4.082	−4.844	1.524	6

indirect energy gap. As can be seen from the Fig. 2, the Fermi level of Pt_1Ni_6 cluster is the highest −4.054 eV, that of Pt_6Ni_1 cluster is the lowest −4.844 eV. The Fermi level is reducing as enhancing the number of Pt atom, indicating that the number of Pt atom determines the fermi level in Pt_nNi_m ($n + m = 7$) clusters. The energy gap of Pt_1Ni_6 and Pt_6Ni_1 are direct energy gap, that of Pt_2Ni_5, Pt_5Ni_2, Pt_3Ni_4 and Pt_4Ni_3 cluster are indirect energy gap. For the same energy level in the Pt_nNi_m ($n + m = 7$) cluster, the energy of down state is higher than that of up state. As to the occupation orbital, the number of up state is always more than that of down state, which is the reason why all the Pt_nNi_m ($n + m = 7$) cluster have magnetic moment.

It is very important to examine the bonding pattern and shape for the chemical reaction via the frontier molecular orbital. That is to say the bonding pattern and shape can reflect the chemical activity and stability of cluster. The HOMO and LUMO maps of Pt_nNi_m ($n + m = 7$) clusters are shown in the Fig. 3. The HOMO of Pt_nNi_m ($n + m = 7$) clusters are mainly attributed to the 5*d* orbital of Pt and 3*d* orbital of Ni atom excluding the s orbital of Ni atom in Pt_2Ni_5 cluster. There is strong *dd*-hybridization in most of HOMO of Pt_nNi_m ($n + m = 7$) clusters, only the *ss*-hybridization between Ni atoms in Pt_2Ni_5 cluster and very weak *dd*-hybridization in Pt_5Ni_2 cluster. For example, there are strong *dd*-hybridization between Ni(2) and Ni(4) atom, as well as Ni(3) and Ni(4) atom in the HOMO of Pt_3Ni_4 cluster. The LUMO of Pt_nNi_m ($n + m = 7$) clusters mainly come from the 5*d* orbital of Pt and 3*d* orbital of Ni atom too, excluding there is existing s orbital in part of Ni atom in Pt_2Ni_5 and Pt_3Ni_4 and Pt_4Ni_3 cluster. In rich Pt and Ni cluster there is strong *dd*-hybridization among the Pt or Ni atom, for example, there are strong *dd*-hybridization among the Ni atoms in Pt_1Ni_6 cluster, as well as that between Pt atoms. But in Pt_2Ni_5, Pt_3Ni_4 and Pt_4Ni_3 clusters, the *sd*-hybridization is obvious due to the existing of s orbital of Pt or Ni atom. For example, there are strong *sd*-hybridization between Ni(2) and Ni(4) atom, Ni(3) and Ni(4), Ni(1) and Pt(5) in Pt_3Ni_4 cluster. The special *sdd*-hybridization among Ni(3), Ni(4), and Ni(5) was in Pt_2Ni_5 cluster. Multifarious orbital hybridization in the frontier molecular orbital can reveal the special electronic structure and provide useful information to experimental study on enhancing its chemical activity definitely.

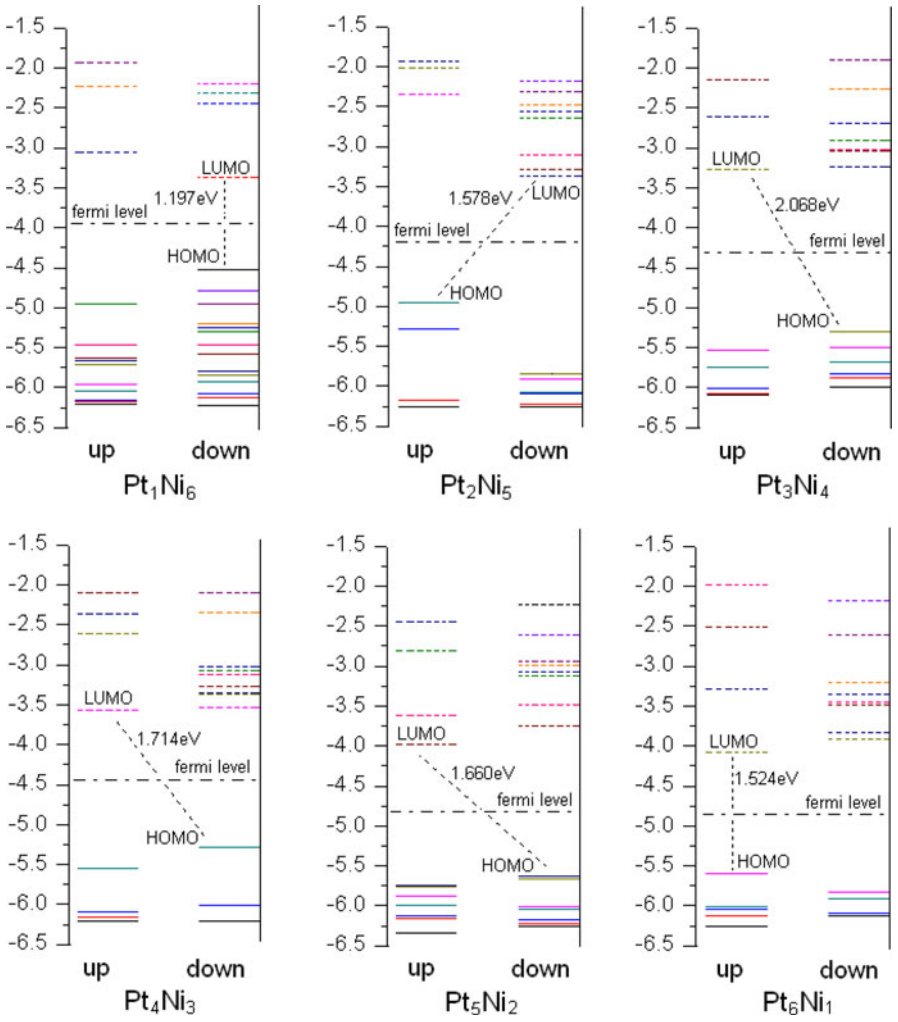

Fig. 2 The partial molecular orbital energy levels of Pt_nNi_m ($n + m = 7$, n, $m \neq 0$) clusters, the '*up*' and '*down*' represent the α- and β-states, respectively

The HOMO–LUMO energy gaps of Pt_nNi_m ($n + m = 7$) clusters are listed in Table 1, which is an important quality to characterize the stability and chemical activity of cluster. The electron in the cluster which has a small energy gap is easy to transfer from HOMO orbital to LUMO orbital, and these clusters have high chemical activity. Large energy gap means high stability. In addition, smaller the energy gap indicates stronger electrical conductivity. As can be seen from Table 1, the energy gap of Pt_nNi_m ($n + m = 7$) clusters shows the increases first and then decreases type change behavior, the energy gap of the Pt_1Ni_6 clusters is the smallest one (1.197 eV), that of the Pt_3Ni_4 cluster is the largest one (2.041 eV), which indicates that the Pt_1Ni_6 cluster has the highest chemical activity and the best

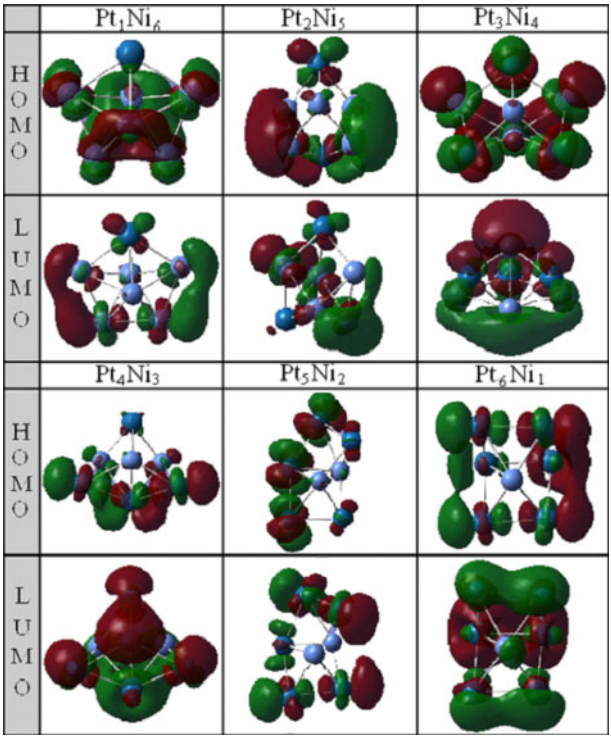

Fig. 3 The frontier molecular orbital pictures of Pt_nNi_m ($n + m = 7$, n, $m \neq 0$) clusters

conductivity. To the contrary, the Pt_3Ni_4 cluster has the lowest chemical activity and the weak conductivity. The energy gap of Pt_6Ni_1 cluster is 1.524 eV, which are little more than Pt_1Ni_6 cluster. The energy gap of Pt_2Ni_5 and Pt_5Ni_2 cluster is 1.578, and 1.660 eV, respectively. This indicates that the rich platinum or nickel cluster have higher chemical activity than others.

Natural Bond Orbital (NBO) Analysis

Table 2 shows the NBO charge populations of Pt_nNi_m ($n + m = 7$, n, $m \neq 0$) clusters. According to the Pauli incompatible principle and lowest energy principle, the configuration of electrons in ground-state atom is consistent with 1*s*, 2*s*, 2*p*, 3*s*, 3*p*, 4*s*, 3*d*, 4*p*, 5*s*, 4*d* order. The formal electron configurations for the Pt and Ni atoms are $5d^9 6s^1$ and $3d^8 4s^2$, respectively. As shown in Table 2, compared with the orbital populations of these formal electron configurations, the populations of 6*s* in few Pt atom and 4*s* in all Ni atom orbitals decrease, whereas the orbital populations of almost all of the 5*d* and 6*p* in Pt atom and 3*d* and 4*p* in Ni atom orbitals increase. For Pt atom in Pt_nNi_m ($n + m = 7$) cluster, the population of 6*s*, and 5*d* and 6*p* orbital range from 0.85 to 1.27, 9.04 to 9.47 and 0.01 to 0.10, respectively. Parts of Pt atoms in some clusters contain the 7*p* and 6*d* orbital, but the population of which are very little. The charge population of Pt atom indicates that the 6*s* in most

Pt atoms and the 5*d* and 6*p* orbital in all Pt atoms orbitals are getting charge, and the orbital hybrid phenomenon has happened between the Pt and Ni atoms or other Pt atoms. For Ni atom in Pt_nNi_m ($n + m = 7$) cluster, the population of 4*s*, 3*d* and 4*p* orbital range from 0.57 to 0.98, 8.60 to 9.02 and 0.02 to 0.11, respectively. Some of Ni atoms located in certain clusters contain the 5*s* and 5*p* orbital, the populations of are very little, just only 0.01. The population of Ni atom demonstrates that the 4*s* orbit is losing charge, the 3*d* and 4*p* orbits are getting charge, and the orbital hybrid phenomenon has happened between the Ni and Pt atoms or other Ni atoms.

Through further analysis of the orbital population of Pt_nNi_m ($n + m = 7$) clusters, we find that the charge gotten by 3*d* and 4*p* and other orbital included are

Table 2 Natural electron configurations and charges of Pt_nNi_m ($n + m = 7$, $n, m \neq 0$) clusters

Cluster	Atom	Natural electron configuration	Charge (e)
Pt_1Ni_6	Ni(1),Ni(3)	4s(0.87)3*d*(8.83)4*p*(0.04)5*s*(0.01)	0.248
	Ni(2),Ni(4)	4s(0.98)3*d*(9.02)4p(0.06)5s(0.01)	−0.071
	Ni(5)	4s(0.73)3*d*(8.97)4*p*(0.09)5*s*(0.01)	0.201
	Ni(6)	4s(0.81)3*d*(8.96)4*p*(0.09)5*s*(0.01)	0.132
	Pt(7)	6s(1.24)5*d*(9.39)6*p*(0.06)	−0.689
Pt_2Ni_5	Ni(1),Ni(2)	4s(0.83)3*d*(8.70)4*p*(0.05)5*s*(0.01)	0.418
	Ni(3),Ni(4)	4s(0.97)3*d*(8.81)4*p*(0.06)5*s*(0.01)	0.161
	Ni(5)	4s(0.92)3*d*(8.87)4*p*(0.07)	0.243
	Pt(6)	6s(1.19)5*d*(9.43)6*p*(0.08)	−0.695
	Pt(7)	6s(1.19)5*d*(9.47)6*p*(0.05)	−0.705
Pt_3Ni_4	Ni(1)	4s(0.58)3*d*(8.64)4*p*(0.05)	0.717
	Ni(2),Ni(3)	4s(0.68)3*d*(8.91)4*p*(0.02)	0.387
	Ni(4)	4s(0.63)3*d*(8.70)4*p*(0.11)5*p*(0.01)	0.556
	Pt(5)	6s(1.27)5*d*(9.44)6*p*(0.08)	−0.786
	Pt(6),Pt(7)	4s(1.17)3*d*(9.42)4*p*(0.05)	−0.631
Pt_4Ni_3	Pt(1),Pt(4)	6s(1.13)5*d*(9.35)6*p*(0.04)	−0.513
	Pt(2)	6s(0.92)5*d*(9.24)6*p*(0.10)6*d*(0.01)	−0.260
	Pt(3)	6s(1.22)5*d*(9.40)6*p*(0.06)	−0.679
	Ni(5)	4s(0.70)3*d*(8.63)4*p*(0.05)	0.613
	Ni(6)	4s(0.57)3*d*(8.64)4*p*(0.06)	0.737
	Ni(7)	4s(0.70)3*d*(8.63)4*p*(0.05)	0.614
Pt_5Ni_2	Ni(1),Ni(2)	4s(0.58)3*d*(8.65)4*p*(0.06)	−0.306
	Pt(3),Pt(5)	6s(0.98)5*d*(9.32)6*p*(0.04)	−0.318
	Pt(4)	6s(0.94)5*d*(9.24)6*p*(0.06)	−0.382
	Pt(6),Pt(7)	6s(0.95)5*d*(9.27)6*p*(0.03)6*d*(0.01)	−0.184
Pt_6Ni_1	Ni(1)	4s(0.59)3*d*(8.60)4*p*(0.08)	0.718
	Pt(2),Pt(6)	6s(0.93)5*d*(9.21)6*p*(0.03)	−0.163
	Pt(3),Pt(4)	6s(0.97)5*d*(9.22)6*p*(0.03)6*d*(0.01)	−0.215
	Pt(5)	6s(0.85)5*d*(9.04)6*p*(0.05)6*d*(0.01)7*p*(0.01)	0.056
	Pt(7)	6s(0.91)5*d*(9.07)6*p*(0.03)6*d*(0.01)	−0.017

less than the charge lost by 4*s* in Ni atom, and the charge gotten by 5*d* and 6*p* and other orbital included are less than the charge lost by 6*s* in Pt atom that adjacent to each Ni atom in the same cluster, which indicates that a few charge are transferred from Ni to Pt atom. To be specific, the charges are transferred from 4*s* of Ni atom to 5*d* of Pt atom. Just because of the interaction between the 4*s* of Ni atom and 5*d* of Pt atom, the Pt–Ni bond is generated and Pt atom gains the charge, which conforms to the atomic electric negative rules (the electronegativity of Pt atom is 2.28 large than that of Ni 1.19) completely. In short, a few transferred charge means orbital hybrid have happened between Pt and Ni atom, which form the chemical bond in cluster and determine the stability and chemical and physical properties. The aforementioned results coincide with the bond pattern and shape of HOMO and LUMO analyzed.

As can be seen from the Table 2 and Fig. 1, the NBO population of Pt_nNi_m ($n + m = 7$) are affected by its symmetry. In some symmetrical clusters, the populations of two atoms that are located in the same relative position are equal. Such as, in the Pt_5Ni_2 cluster whose symmetry is C_2, the population of Ni(1) and Ni(2), Pt(3) and Pt(5), Pt(6) and Pt(7) are $4s^{0.58}3d^{8.65}4p^{0.06}$, $6s^{0.98}5d^{9.32}6p^{0.04}$ and $6s^{0.95}5d^{9.27}6p^{0.03}6d^{0.01}$ respectively. The net charge of every atom in Pt_nNi_m ($n + m = 7$) cluster gained by using NBO method are also shown in Table 2. The net charge range from −0.786e to +0.056e for Pt atom, and range from −0.306e to +0.737e for Ni atom, this indicates that the charge adjustable ability of Ni is stronger than Pt atom and the Ni is easier to combine with other atom than Pt atom to form chemical bond. This conclusion is also consist with the atomic electric negative rules previous mentioned.

Spectrum Analysis

It is necessary to make comparison between the experimentally obtained spectra and simulated spectra to determine the cluster structures by diffraction. In this article, we use B3LYP/LANL2DZ method to calculate the infrared and Raman spectra for the ground state structures of Pt_nNi_m ($n + m = 7$, n, $m \neq 0$) clusters, which is able to interpret the spectra in terms of the cluster structures once the experimental spectra have been recorded. In the IR spectrum, the unit of horizontal ordinate is (cm^{-1}) and that of vertical coordinates is (KM/Mol). As to the Raman spectrum, the unit of horizontal ordinate is (cm^{-1}) and that of vertical coordinates is (A^4/AMU).

As shown in Fig. 4, for Pt_1Ni_6 cluster, there are three obvious peaks in IR spectrum, the strongest peak at 162.42 cm^{-1} is mainly assigned to swing of Ni(5) and Ni(6) atom synchronous; two second strong peaks are located at 108.86 and 186.45 cm^{-1}, the vibration mode of the former is the asynchronous stretching between the Ni(1) and Ni(2) atom, Ni(3) and Ni(4) atom fixed in the joints of the middle pentagon, the latter whose vibration mode is the asynchronous stretching between the Ni(2) and Ni(4) atom fixed in the joints of the pentagon. As to its Raman spectrum, the strongest peak is at 249.95 cm^{-1}, whose vibration mode is the stretching of the Ni(5) and Ni(6) atom fixed in the two vertex of the pentagonal bipyramid. The second strong peak is at 239.02 cm^{-1}, whose vibration mode is the stretching of the Ni(2) and Ni(3) atom.

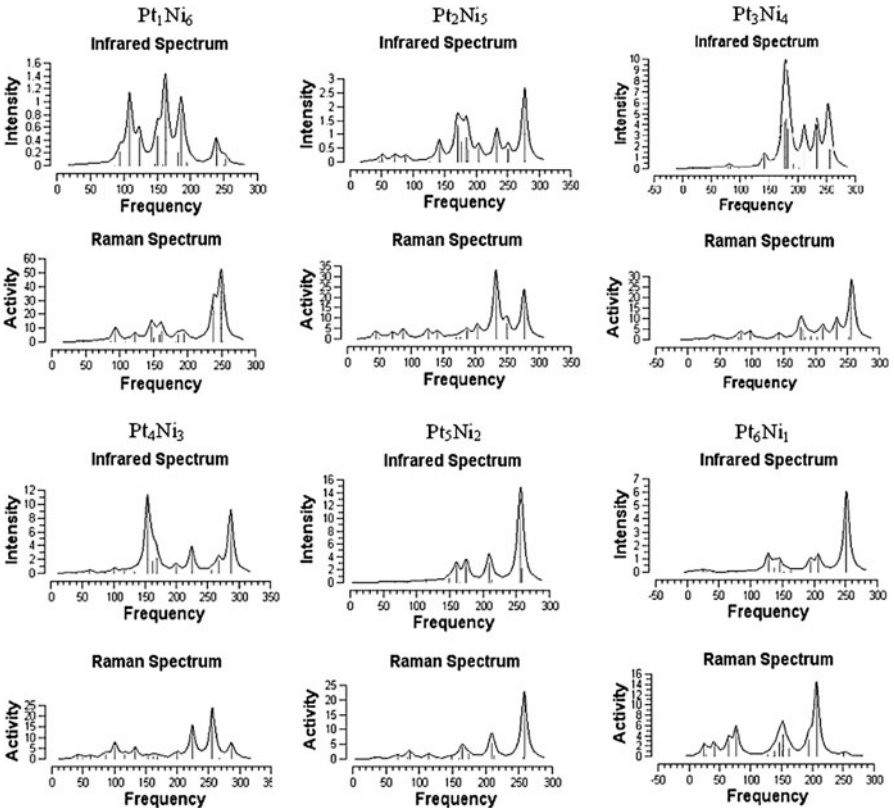

Fig. 4 Infrared and Raman spectra of Pt_nNi_m ($n + m = 7$, $n, m \neq 0$) clusters at ground state

For Pt_2Ni_5 cluster, there are five obvious peaks in the IR spectrum, the strongest peak assigned to stretching of the Ni(1), Ni(2) and Ni(5) atom in-plane is at 277.12 cm^{-1}; the second peak mainly assigned to the swing of the Ni(5) atom is at 170.17 cm^{-1}; and the third peak is at 233.04 cm^{-1}, whose vibration mode is the strong stretching of Pt(7) atom. In the Raman spectrum of Pt_2Ni_5 cluster, there are two obvious peaks, the strongest one is at 233.04 cm^{-1}, whose vibration mode is the same with that of its IR spectrum at this point. The second peak is at 277.12 cm^{-1}, whose vibration mode is that of its IR spectrum.

For Pt_3Ni_4 cluster, there are four obvious peaks in the IR spectrum, the strongest peak assigned to stretching and swing of the Ni(1), Ni(2), Ni(3) and Ni(4) atom at 179.24 cm^{-1} is a three-degenerate peak; the second peak assigned to strong swing of Ni(1) and Ni(4) atom is at 252.48 cm^{-1}; and the third peak is at 233.35 cm^{-1}, whose vibration mode is mainly the stretching of the Pt(5) atom. As to its Raman spectrum, the strongest peak is at 256.86 cm^{-1}, whose vibration mode is the stretching of the Pt(6) and Pt(7) atom. The other peaks are very weak and will not be described here.

For Pt_4Ni_3 cluster, there are three obvious peaks in the IR spectrum, the strongest peak is at 154.04 cm^{-1}, which is assigned to stretching of the Ni(5), Ni(6), Ni(7), Pt(1) and Pt(4) atoms in three-dimension space; the second peak is at 286.91 cm^{-1}, whose vibration mode is mainly the synchronous stretching of the middle Ni(5), Ni(6) and Ni(7) atom; and the third peak at 224.45 cm^{-1} is a relative weak one. As to its Raman spectrum, the strongest peak is at 256.60 cm^{-1}, whose vibration mode is the vibration of the Ni(5) and Ni(7) atom up and down in plane defined by Pt(2), Ni(6) and Pt(3) atom. The second peak is at 224.45 cm^{-1}, whose vibration mode is consist with that of IR spectrum.

For Pt_5Ni_2 cluster, there are four obvious peaks in the IR spectrum, the strongest peak assigned to stretching vibration of the Ni(1), Ni(2), Pt(4) toward to the two direction of Pt(3)–Pt(6) and Pt(5)–Pt(7) bond, respectively is at 256.22 cm^{-1}; the second peak is at 209.74 cm^{-1}, whose vibration mode is the swing of Ni(1) and Ni(2) atoms. The intensity of other two peaks is approximate to the second peak. In the Raman spectrum of Pt_5Ni_2 cluster, there are three obvious peaks, the strongest one is at 257.85 cm^{-1}, whose vibration mode is the stretching vibration of the Ni(1) and Ni(2) atom up and down in plane defined by Pt(4), Ni(6) and Pt(7) atom. the second peak is at 208.50 cm^{-1}, whose vibration mode is stretching of the Ni(1) and Ni(2) atom.

For Pt_6Ni_1 cluster, there are five obvious peaks in the IR spectrum, the strongest peak at 251.04 cm^{-1} is assigned to stretching vibration of the Ni(1) atom toward to the bilateral Pt atom; the other peaks are at 127.72, 206.80, 145.79 and 194.18 cm^{-1}, whose vibration mode are the stretching of Ni(1) atom to different direction in space. In the Raman spectrum of Pt_6Ni_1 cluster, there are six obvious peaks, the strongest one is at 206.80 cm^{-1}, whose vibration mode is the internal and external expansion of the Ni(1) atom. The second peak is at 152.97 cm^{-1}, whose vibration mode is stretching of the Ni(1), Pt(2), Pt(5), Pt(6) and Pt(7) atom.

In general, there are many obvious peaks in all the IR and Raman spectrum of Pt_nNi_m ($n + m = 7$) cluster, whose position are distinct. The strongest peak in IR spectrum is located at above 150 cm^{-1}, that of Raman spectrum are above 200 cm^{-1}. In the low frequency position, the peaks of both IR and Raman spectrum are little and small.

Aromatic Properties

The aromaticity of organic compounds has been studied extensively. As the widely spread of aromaticity, the study of the aromaticity to the metal clusters of inorganic compounds increased, but there were few application to the transition-metal clusters. The aromatic characterization of the clusters shows strong magnetic shielding effect, big ring current, and big resonance energy, and other special properties, these properties make them have a potential application in nonlinear optical materials, the conductor, catalyst and adsorption etc. In this research, the ground states of Pt_nNi_m ($n + m = 7$, n, $m \neq 0$) clusters were investigated by using GIAO-B3LYP/LANL2DZ methods implanted in the Gaussian 03 package. The concept of NICS was introduced by Schleyer et al. [28, 29] in 1996 as a measure of aromaticity and antiaromaticity (or nonaromaticity) NICS is also a simple and

Table 3 Nucleus independent chemical shifts (NICS) of Pt_nNi_m ($n + m = 7$, $n, m \neq 0$) cluster

Cluster	Structure	NICS/10^{-6}				
		Site *A*	Site *B*	Site *C*	Site *D*	Site *E*
Pt_1Ni_6	a	−17.767	1.107	−1.129	−4.741	−0.243
Pt_2Ni_5	b	−38.214	−34.093	−31.139	−15.077	−14.924
Pt_3Ni_4	c	−25.150	−25.126	−23.637	−18.032	−24.195
Pt_4Ni_3	d	−37.152	−26.478	−10.126	−17.670	−21.710
Pt_5Ni_2	e	−28.892	−27.398	−24.420	−22.652	−14.152
Pt_6Ni_1	f	−58.644	−43.270	−33.019	−29.155	28.586

effective criterion to probe two- and three-dimensional aromaticity. It is based on a probe with no basis function (Bq) which is placed at or above the geometrical center of a conjugated ring. They suggested that the probe (Bq) should be placed at the center or 1 Å above the molecular planes of systems. Generally, aromaticity is charactered by a negative NICS value (given in ppm), antiaromaticity by a positive NICS value and NICS value of a nonaromaticity compound is close to zero. The NICS of Pt_nNi_m ($n + m = 7$) are measured by five reference points, point *A* is located in the center of triangular prism, points *B*, *C*, *D*, *E* are situated at the vertical distance of 0.25, 0.50, 0.75 and 1.00 Å place away from the plane or profile plane (abbreviation: plane), respectively.

As can be seen from Table 3, all the Pt_nNi_m ($n + m = 7$) clusters have aromaticity. At the site *E* and B, the Pt_1Ni_6 cluster has nonaromaticity, the Pt_6Ni_1 has antiaromaticity at the site E. The aromatic degrees of Pt_2Ni_5, Pt_5Ni_2 and Pt_6Ni_1 are decreasing from the center (*A*) to outlying area (*E*). More information is followed. The absolute value of NICS in Pt_6Ni_1 cluster is the biggest in the site *A*, *B*, *C* and *D* in all the Pt_nNi_m ($n + m = 7$) clusters when we put a probe atom Bq in these site, which indicates that the Pt_6Ni_1 cluster has the strongest aromaticity. When the probe atom Bq is put at the site *E* of Pt_6Ni_1 cluster, its NICS value becomes positive successive, which suggests that this cluster has antiaromaticity because there is the shielding effect of σ bond. When the probe atom Bq is put at the site *E* and *B* of Pt_1Ni_6 cluster, the NICS value approximated to zero, which demonstrates those two points have nonaromaticity. The negative degrees of NICS value in Pt_2Ni_5, Pt_5Ni_2 and Pt_6Ni_1 are decreasing as putting the probe atom Bq at from site *A* to site *E*, which indicates that the aromatic degrees of this three clusters are reducing. It can be explained that the aromaticity is reduced when the delocalized electron decreases at the site away from the center of this cluster. To deeply research the abnormal condition of Pt_1Ni_6, Pt_3Ni_4 and Pt_4Ni_3 clusters, we study on the electronic structure and chemical bond of Pt_nNi_m ($n + m = 7$) clusters and conclude that the aromaticity of Pt_nNi_m ($n + m = 7$) clusters are directly bound up with its geometric structure. As to the regular geometric structure, such as cage and ring, the reference point (*A*) are locate at the geometric center. When the probe atom Bq is put at the site *A*, *B*, *C*, *D* and *E* successively, the NICS values are going to decrease uniformly step by step due to reduction of the delocalized electrons

caused by the minishing combining effect of ring current gradual formed by different orbital hybridization, especially the *d* electron orbital contained. So it is not difficult to understand the abnormal change of the NICS value in the Pt_1Ni_6, Pt_3Ni_4 and Pt_4Ni_3 clusters. It is found that the aromaticity of the transition-metal clusters is stronger than that of the organic and inorganic clusters because there are contributions from *d* orbitals for the transition-metal clusters.

Conclusion

In this work, we give a systematic theoretical study of Pt_nNi_m ($n + m = 7$, n, $m \neq 0$) clusters using the DFT method. Based on the carefully optimized geometries, we have calculated the energy level, NBO, the infrared and Raman spectrum, and the aromatic properties for the Pt_nNi_m ($n + m = 7$) clusters. The results are summarized as follows:

(a) The ground state structures of Pt_nNi_m ($n + m = 7$, n, $m \neq 0$) clusters are all three-dimensional structures, which are irregular structures with low symmetry and high spin multiplicity.

(b) The detailed energy level and natural (NBO) charge analyses indicate that the Fermi level is determined by the number of Pt atoms, and Pt_1Ni_6 and Pt_6Ni_1 clusters have a direct energy gap. Multifarious orbital hybridization is found in the frontier molecular orbital and the rich platinum or nickel cluster have smaller energy gap than others. The charge is mainly transferred from Ni atoms to Pt atoms, which brings about strong orbital hybrid phenomenon and high chemical activity in Pt_nNi_m ($n + m = 7$) clusters.

(c) From the infrared and Raman spectra of Pt_nNi_m ($n + m = 7$) clusters, we can see that there are many obvious peaks in all the IR and Raman spectrum, the strongest peaks of IR spectrum are located at above 150 cm^{-1}, that of Raman spectrum are above 200 cm^{-1}. In the low frequency position, the peaks of both IR and Raman spectrum are little and small.

(d) All of PtnNim ($n + m = 7$) clusters have aromaticity, except Pt_1Ni_6 and Pt_6Ni_1 cluster. The aromatic degree of Pt_2Ni_5, Pt_5Ni_2 and Pt_6Ni_1 is decreasing from the center to outlying area. The aromaticity is highly correlated to its geometric structure, and the electronic structure especially the *d* orbitals for the transition-metal clusters are very important to their aromaticity.

Acknowledgment Project supported by the National Natural Science Foundation of China (Grant No. 51072072); Project supported by the Natural Science Foundation of Jiangsu Province (BK2010343).

References

1. R. Ferrando, J. Jellinek, and R. L. Johnston (2008). *Chem. Rev.* **108**, 845.
2. B. S. Mun, M. Watanabe, M. Rossi, V. Stamenkovic, N. M. Markovic, and J. Ross (2005). *J. Chem. Phys.* **123**, 204717.
3. Y. S. Lee, J. Y. Rhee, C. N. Whang, and Y. P. Lee (2003). *Phys. Rev. B Condens. Matter Mater. Phys.* **68**, 235111.

4. C. E. Mary, G. Elod, N. Hiroshi, and K. Hideaki (2011). *J. Nanosci. Nanotech.* **11**, 4.
5. J. N. Zhang, S. J. You, Y. X. Yuan, Q. L. Zhao, and G. D. Zhang (2011). *J. Electrochem. Com.* **13**, 9.
6. L. Xiong and A. Manthiram (2004). *Electrochim. Acta.* **49**, 4163.
7. H. Yano, M. Kataoka, H. Yamashita, H. Uchida, and M. Watanabe (2007). *Langmuir.* **23**, 6438.
8. S. Koh, J. Leisch, M. F. Toney, and P. Strasser (2007). *J. Phys. Chem. C.* **111**, 3744.
9. V. Stamenkovic, B. S. Mun, K. J. J. Mayrhofer, P. N. Ross, N. M. Markovic, J. Rossmeisl, J. Greeley, and J. K. Nøskov (2006). *Angew Chem. Int. Ed.* **45**, 2897.
10. E. Antolini, J. R. C. Salgado, and E. R. Gonzalez (2006). *J. Power Sources.* **160**, 957.
11. J. K. Nøskov, J. Rossmeisl, A. Logadottir, L. Lindqvist, J. R. Kitchin, T. Bligaard, and H. Jónsson (2004). *J. Phys. Chem. B.* **108**, 17886.
12. A. Kootte, C. Haas, and R. A. de Groot (1991). *J. Phys. Condens. Matter.* **3**, 1133.
13. L. Xiong and A. Manthiram (2005). *J. Electrochem. Soc.* **152**, A697.
14. L. Xiong and A. Manthiram (2004). *J. Mater. Chem.* **14**, 1454.
15. X. R. Zhang, L. L. Hong, and C. H. Gao (2009). *J. Atom. Mol. Phys.* **26**, 257. (in Chinese).
16. X. R. Zhang, C. H. Gao, and L. L. Hong (2009). *Acta Photonica Sinica.* **38**, 3109. (in Chinese).
17. X. R. Zhang, X. Yang, Y. Li, and W. L. Guo (2011). *Acta Photonica Sinica.* **69**, 2063. (in Chinese).
18. M. J. Frisch, et al. *GAUSSIAN 03* (Gaussian, Inc, Pittsburgh, PA, 2003).
19. P. J. Hay and W. R. Wadt (1985). *J. Chem. Phys.* **82**, 299.
20. X. R. Zhang, X. L. Ding, B. Dai, and J. L. Yang (2005). *J. Mol. Struct. Theochem.* **757**, 113.
21. X. R. Zhang, X. L. Ding, and J. L. Yang (2005). *Int J. Mod. Phys. B.* **19**, 2427.
22. X. R. Zhang, X. L. Ding, Q. Fu, and J. L. Yang (2008). *J. Mol. Struct. Theochem.* **867**, 17.
23. M. B. Airola and M. D. Morse (2002). *J. Chem. Phys.* **116**, 1313.
24. J. C. Fabbi, J. D. Langenberg, Q. D. Costello, M. D. Morse, and L. Karlsson (2001). *J. Chem. Phys.* **115**, 7543.
25. S. Taylor, G. W. Lemire, Y. M. Hamrick, Z. Fu, and M. D. Morse (1988). *J. Chem. Phys.* **89**, 5517.
26. H. M. Yin, H. M. Duan, and X. J. Zhao (2009). *J. Sichuan Univ. Nat. Sci.* **45**, 605. (in Chinese).
27. H. Q. Sun, Y. Ren, and G. H. Wang (2001). *J. Atom. Mol. Phys.* **18**, 387. (in Chinese).
28. P. V. R. Schleyer, H. Jiao, N. V. E. Hommes, V. G. Malkin, and O. L. Malkina (1997). *J. Am. Chem. Soc.* **119**, 12669.
29. P. V. R. Schleyer, C. Maerker, A. Dransfeld, H. Jiao, and N. J. R. V. E. Hommes (1996). *J. Am. Chem. Soc.* **118**, 6317.